RNA–Protein Complexes

DOI: 10.1002/anie.201301411

The Structure of $FemX_{Wv}$ in Complex with a Peptidyl-RNA Conjugate: Mechanism of Aminoacyl Transfer from Ala-$tRNA^{Ala}$ to Peptidoglycan Precursors**

Matthieu Fonvielle, Inés Li de La Sierra-Gallay, Afaf H. El-Sagheer, Maxime Lecerf, Delphine Patin, Dénia Mellal, Claudine Mayer, Didier Blanot, Nittaya Gale, Tom Brown, Herman van Tilbeurgh, Mélanie Ethève-Quelquejeu, and Michel Arthur**

Further to protein synthesis by the ribosome, aminoacyl-tRNAs participate as donors of activated aminoacyl residues in various biosynthetic pathways, including assembly of the side chain of peptidoglycan precursors by aminoacyl transferases of the Fem family.[1,2] The latter enzymes are attractive targets for drug development, as they have no counterpart in mammalian cells and perform essential steps in cell-wall assembly in important multidrug-resistant pathogens, such as *Staphylococcus aureus*, *Streptococcus pneumoniae*, and *Enterococcus faecalis*. $FemX_{Wv}$ from *Weissella viridescens*, a model enzyme for the Fem family, catalyzes transfer of L-Ala from Ala-$tRNA^{Ala}$ to the side-chain amine of L-Lys present at the third position of the peptidoglycan precursor UDP-MurNAc-pentapeptide (Scheme 1 A).

The structure of $FemX_{Wv}$ has been previously determined both for the apo form and for complexes containing UDP-MurNAc-pentapeptide[3] (PDB code 1P4N) or the product of the reaction UDP-MurNAc-pentapeptide(Ala) (PDB code 3GKR). Co-crystallization with RNA has been unsuccessful, which is presumably due to the low affinity of $FemX_{Wv}$ for free $tRNA^{Ala}$,[4] instability of the Ala-$tRNA^{Ala}$ ester bond, and ordered fixation of the substrates,[5] that is, the peptidoglycan precursor followed by Ala-$tRNA^{Ala}$, which hinders formation

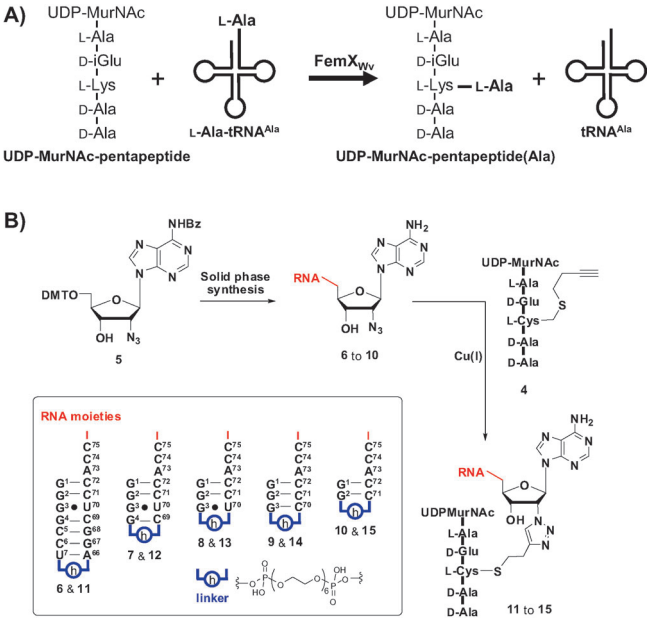

Scheme 1. A) Aminoacyl transfer reaction catalyzed by $FemX_{Wv}$. B) Synthesis of peptidyl-RNA conjugates. Structure of peptidyl-RNA conjugates. Base numbering refers to $tRNA^{Ala}$.

[*] Dr. M. Fonvielle,[+] M. Lecerf, Dr. C. Mayer, Dr. M. Arthur
Laboratoire de Recherche Moléculaire sur les Antibiotiques
Centre de Recherche des Cordeliers, Equipe 12, INSERM, U872
75006 Paris (France)
and
Université Pierre et Marie Curie – Paris 6, UMR S 872
15 rue de l'Ecole de Médecine, 75006 Paris (France)
and
Université Paris Descartes, Sorbonne Paris Cité, UMR S 872
75006 Paris (France)
E-mail: michel.arthur@crc.jussieu.fr

Dr. I. Li de La Sierra-Gallay,[+] Dr. H. van Tilbeurgh
Fonction et Architecture des Assemblages Macromoléculaires
Institut de Biochimie et de Biophysique Moléculaire et Cellulaire
Université Paris-Sud, UMR 8619, 91405 Orsay (France)

Dr. A. H. El-Sagheer
Chemistry Branch, Dept. of Science and Mathematics
Faculty of Petroleum and Mining Engineering
Suez University, Suez, 43721 (Egypt)

D. Patin, Dr. D. Blanot
Laboratoire des Enveloppes Bactériennes et Antibiotiques
Institut de Biochimie et de Biophysique Moléculaire et Cellulaire
Université Paris-Sud, UMR 8619, 91405 Orsay (France)

Dr. D. Mellal, Dr. M. Ethève-Quelquejeu
Laboratoire de Chimie et de Biochimie Pharmacologiques et Toxicologiques, Université Paris Descartes
UMR 8601, 75270 Paris (France)
and
CNRS, UMR 8601, 75270 Paris (France)
E-mail: melanie.etheve-quelquejeu@parisdescartes.fr

Dr. A. H. El-Sagheer, Dr. N. Gale, Dr. T. Brown
School of Chemistry, University of Southampton
Highfield, Southampton, SO17 1BJ (UK)

Dr. I. Li de La Sierra-Gallay,[+] D. Patin, Dr. D. Blanot, Dr. H. van Tilbeurgh
CNRS, UMR 8619, 91405 Orsay (France)

[+] These authors contributed equally to this work.

[**] This work was supported by the European Community (EUR-INTAFAR, Project No. LSHM-CT-2004-512138, 6th PCRD), and the French Infrastructure for Integrated Structural Biology (FRISBI) ANR-10-INSB-05-01, and a UK BBSRC sLOLA grant to A.H.E.-S. and T.B. (BB/J001694/1 "Extending the boundaries of nucleic acid chemistry"). D.M. was supported by a research fellowship from the Région Ile-de-France. We thank the PROXIMA 1 staff for help with synchrotron data collection.

Supporting information for this article is available on the WWW under http://dx.doi.org/10.1002/anie.201301411.

of a binary Fem/Ala-tRNA^{Ala} complex. We have now synthesized stable peptidyl-RNA conjugates mimicking the two substrates of FemX$_{Wv}$. These compounds are composed of a peptidoglycan precursor analogue covalently linked to RNA moieties mimicking the acceptor arm of tRNA^{Ala}. The convergent method for synthesis of these "bi-substrates" (Scheme 1 B) is based on copper-assisted cycloaddition between alkyne UDP-MurNAc-pentapeptide **4** and 2′-azido RNA duplexes **6** to **10**, which contain 2 to 7 base pairs. As duplexes containing less than five base pairs are unstable in solution, we connected RNA strands by a hexaethylene glycol linker[6,7] (Scheme 1 B). tRNA^{Ala} analogues **6** to **10** were obtained by phosphoramidite solid-phase synthesis starting with azido-functionalized adenosine **5** (Supporting Information, Scheme 1). Peptidoglycan-precursor analogue **4** was obtained by semi-synthesis.[8] The Cu^{I}-catalyzed azide–alkyne cycloaddition reaction (Cu-AAC)[9,10] afforded "bi-substrate" analogues **11** to **15** containing RNA and peptidoglycan-precursor moieties connected by a 1,4-triazole ring.

We have previously introduced deletions in Ala-tRNA^{Ala} and showed that the acceptor arm is sufficient for efficient and specific transfer of Ala to the peptidoglycan precursor.[11] To further evaluate the role of the acceptor-arm base pairs in substrate recognition, we assayed peptidyl-RNA conjugates **11** to **15** as inhibitors of FemX$_{Wv}$ aminoacyl-transferase activity (Supporting Information, Figure S2). Compound **11**, which contained the full complement of the seven base pairs present in the tRNA^{Ala} acceptor arm, inhibited FemX$_{Wv}$ at a subnanomolar concentration ($IC_{50} = 0.15 \pm 0.01$ nM). Decreasing the base-pair number from 7 to 4, 3, and 2 resulted in an increase in IC_{50} (2.0 ± 0.2, 100 ± 10, and 930 ± 70 nM, respectively). Substitution of base pair G^3U^{70} (**13**) by GC (**14**) decreased the IC_{50} from 100 ± 10 to 35 ± 1 nM. Together, these results indicate that the double-stranded RNA moiety is critical for binding of peptidyl-RNA conjugates to FemX$_{Wv}$ and that the four proximal base pairs of the acceptor arm are sufficient for high affinity.

FemX$_{Wv}$ was successfully co-crystallized with peptidyl-RNA conjugate **15**. The final 1.66 Å structure includes all FemX$_{Wv}$ residues, the UDP-MurNAc-pentapeptide, triazole ring, and terminal CCA moieties of **15** (see the Supporting Information, Table S1 for statistics). The electron-density map of **15** was well-defined in the FemX$_{Wv}$ catalytic cavity (Figure 1 A). The UDP-MurNAc-pentapeptide moiety of **15** was located at the interface of the two FemX$_{Wv}$ domains, which both display a GCN5-related *N*-acetyltransferase (GNAT) fold (Figure 1 B), as previously described for FemX$_{Wv}$ in complex with UDP-MurNAc-pentapeptide[3] and UDP-MurNAc-pentapeptide(Ala). The latter structures differ solely at the level of the L-Lys side chain, which is only defined following addition of Ala. The RNA moiety of **15** occupies the long channel running across domain 2 (Supporting Information, Figure S3). The structures of FemX$_{Wv}$ in complex with **15** and UDP-MurNAc-pentapeptide(Ala) could be superimposed with an RMSD value of 0.423 Å for 332 residues in common, indicating the absence of overall changes in the protein conformation, except in the loops connecting strands β5 and β6 and helices α6 and α7.

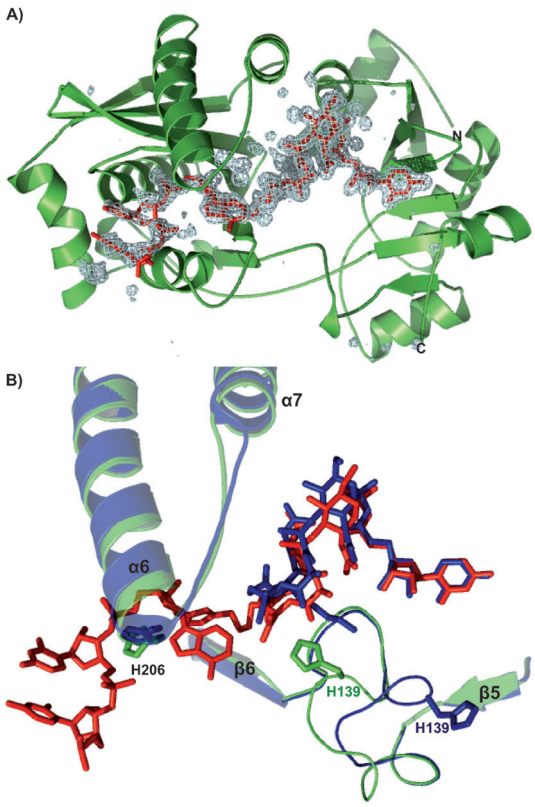

Figure 1. A) Complex formed by FemX$_{Wv}$ (green) with peptidyl-RNA conjugate **15** (red sticks). 3σ residual difference density was calculated with the buster program and with an input PDB file not containing any ligand atoms. B) Superposition of **15** (red)/FemX$_{Wv}$ (green) and UDP-MurNAc-pentapeptide(Ala) (blue)/FemX$_{Wv}$ (light blue) complexes.

In comparison to the FemX$_{Wv}$-UDP-MurNAc-pentapeptide(Ala) complex, binding of **15** led to concerted rearrangements in the β5-β6 loop of FemX$_{Wv}$ and in the L-Ala^1-D-iGlu^2-L-Cys^3 moiety of **15**, including a 129° rotation of the L-Lys^3 Cα-Cβ bond (Supporting Information, Figure S4). Residues 136–140 within loop β5-β6 of FemX$_{Wv}$, originally in contact with the solvent, flip into the catalytic cavity (Figure 1 B), resulting in new contacts between the protein and the pentapeptide stem (Figure 2). In particular, the His139 imidazole ring establishes hydrogen-bonding interactions with the carbonyl and carboxyl groups of D-iGlu^2 and N^1 of A^{76} through a bridging water molecule (Figure 3 A). These interactions are critical in fixing the side-chain position of L-Lys^3, which points to the opposite side of the cavity in the FemX$_{Wv}$/UDP-MurNAc-pentapeptide(Ala) complex (Inset in Figure 2; Supporting Information, Figure S4).

Multiple interactions were detected between the CCA extremity of peptidyl-RNA conjugate **15** and FemX$_{Wv}$. The Ile208 side chain moved by 2.2 Å upon binding of **15** to establish a hydrophobic interaction with the terminal adenine, which was also in contact with Leu301 (Figure 3 B). The Ile208Ala substitution led to a 50-fold decrease in turnover number. The phosphates of the 3′ terminal C^{75} and A^{76} nucleotides of **15** are stabilized by a hydrogen-bonding network involving Arg205, Ser259, and His206. His206 rotates by 90° and moves by 1.6 Å toward the inside of the

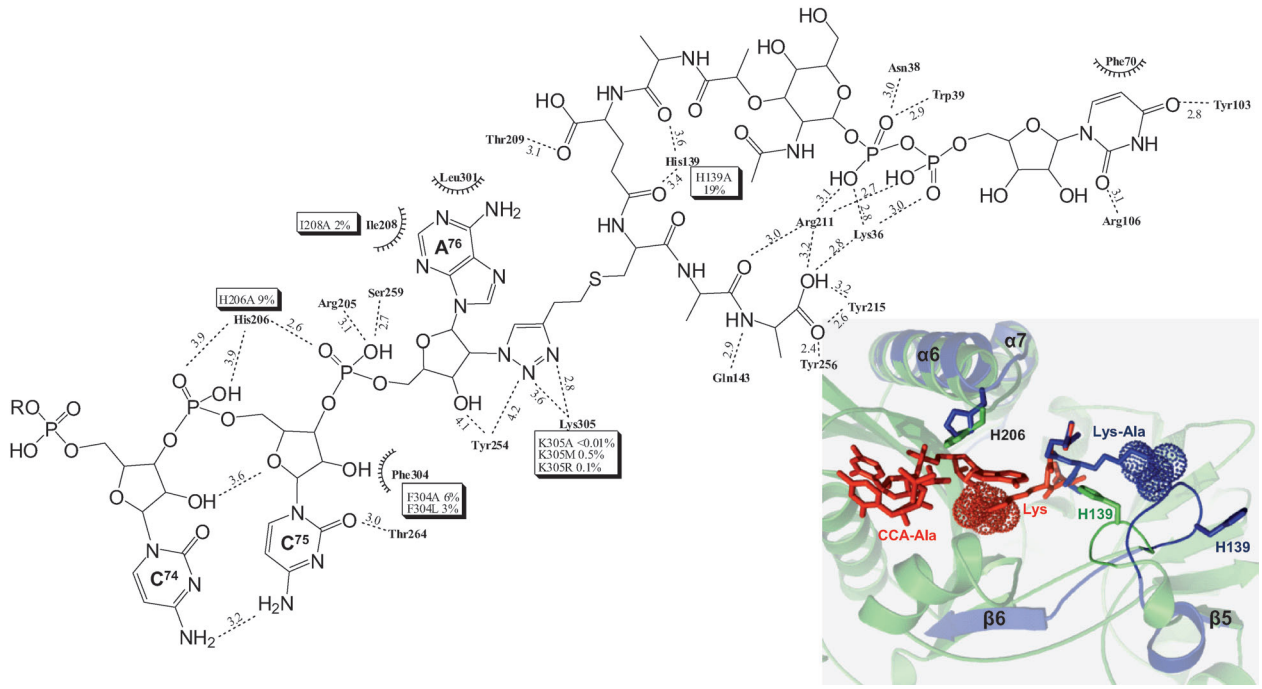

Figure 2. Interaction map of peptidyl-RNA conjugate **15** bound to $FemX_{Wv}$. Turnover numbers for derivatives of $FemX_{Wv}$ harboring various amino acid substitutions are indicated as percentages relative to wild-type enzyme. Residual activities for the complete set of substitutions are presented in the Supporting Information, Table S2. Inset: Superposition of the $FemX_{Wv}$/UDP-MurNAc-pentapeptide(Ala) complex and a model of the two substrates in the $FemX_{Wv}$ catalytic cavity. In the complex, $FemX_{Wv}$ is shown in gray blue and the D-iGlu-L-Lys(L-Ala)-D-Ala moiety of UDP-MurNAc-pentapeptide(Ala) is shown in blue with Ala highlighted by blue spheres. The model includes $FemX_{Wv}$ (green), the D-iGlu-L-Lys-D-Ala moiety of UDP-MurNAc-pentapeptide (beige), and the CCA-Ala extremity of Ala-$tRNA^{Ala}$ (red) with Ala highlighted by red spheres.

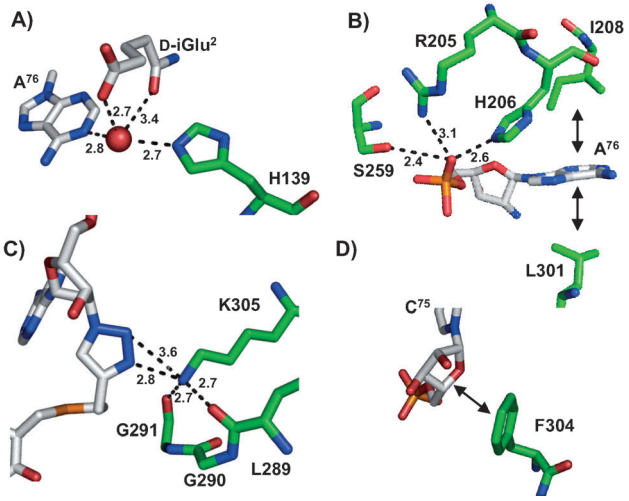

Figure 3. Interactions between $FemX_{Wv}$ and the RNA moiety of **15**. A) Hydrogen-bonding interactions between His139, D-$iGlu^2$, and A^{76}. The red sphere represents a water molecule. B) Hydrogen-bonding interactions between the A^{76} phosphate group, Ser259, Arg205, and His206. Black arrows represent hydrophobic interactions between A^{76} and residues Ile208 and Leu301. C) Triazole ring of **15** in interaction with Lys305 of $FemX_{Wv}$. D) Phe304 interaction with C^{75} ribose.

catalytic cavity. This movement is critical for formation of three hydrogen-bonding interactions with the phosphates of C^{75} and A^{76}. The critical role of these interactions for optimal $FemX_{Wv}$ activity is shown by the 11-fold reduction in the turnover number caused by the His206Ala substitution.

The crystal structure of $FemX_{Wv}$ in complex with **15** enables localization of putative active-site residues, as the triazole ring, which is an isostere of an ester bond,[12–14] identifies the position of the reacting Ala-$tRNA^{Ala}$ ester bond during catalysis. Lys305, whose side-chain amine is in hydrogen-bonding distance with N^3 from the triazole ring (Figure 3C), was identified as the sole $FemX_{Wv}$ residue that could participate in the chemical step of the reaction. Lys305 of $FemX_{Wv}$ and the preceding residue, Phe304, are highly conserved in Fem aminoacyl transferases (Supporting Information, Figure S5).[3] Lys305 is in hydrogen-bonding distance with the carbonyl groups of Gly291 and Leu289, both in the free form of the enzyme and in the complexes containing peptidyl-RNA conjugate **15**, UDP-MurNAc-pentapeptide, or UDP-MurNAc-pentapeptide(Ala). Substitution of Lys305 by Ala, Met, or Arg decreased turnover number 1.3×10^4, 1.9×10^2, and 9.9×10^2-fold, respectively. The position of Lys305 and its critical role for optimal activity indicate that the amine of this conserved residue may stabilize the negative charge that develops on the carbonyl of L-Ala upon nucleophilic attack of the Ala-$tRNA^{Ala}$ ester bond by the amine of Lys^3. Phe304, is also critical for activity, as the Phe304Ala and Phe304Leu substitutions decreased the $FemX_{Wv}$ turnover number 16 and 29-fold, respectively. These substitutions disrupt the π stacking interaction with the C^{75} ribose (Figure 3D). As Lys305 is the only reactive amino acid in the vicinity of the triazole ring, the enzyme does not contribute to aminoacyl transfer by providing a catalytic base or acid, indicating that catalysis proceeds by a substrate-assisted

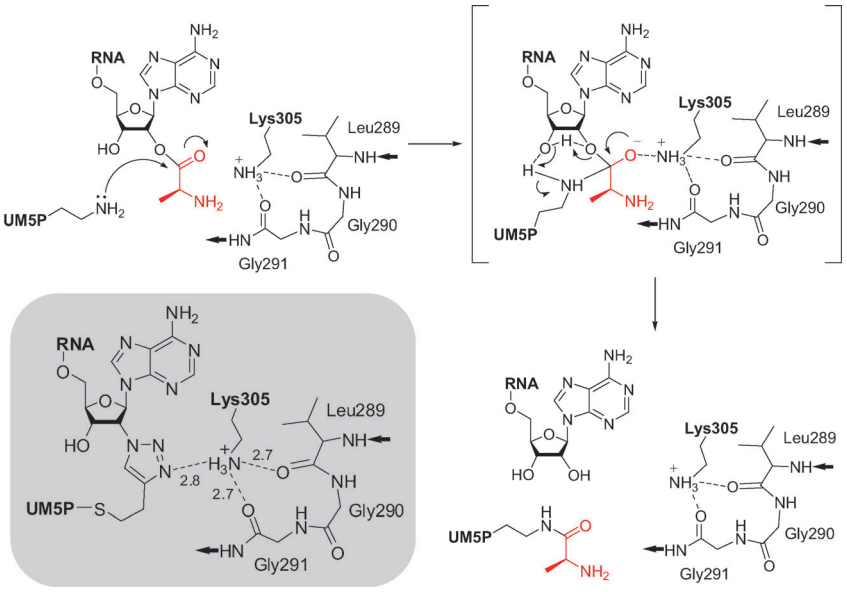

Scheme 2. Model for the aminoacyl transfer reaction. UM5P, UDP-MurNAc-pentapeptide. The gray inset shows the triazole ring of **15** in interaction with $FemX_{Wv}$. The proton shuttle mechanism proposed for $FemX_{Wv}$ has also been considered for the ribosome, although recent evidence rules out this concerted mechanism and identified the negatively charged tetrahedral adduct (T^-) as a key reaction intermediate.[15]

mechanism (Scheme 2). In agreement, the tRNA terminal 3′-hydroxy group is essential for efficient aminoacyl transfer from the 2′-position but not for binding of Ala-$tRNA^{Ala}$ to $FemX_{Wv}$.[4]

In conclusion, the structure-based mechanism for peptide-bond formation by $FemX_{Wv}$ involves a combination of protein-induced stabilization of the negative charge that develops in the tetrahedral intermediate and substrate-assisted proton shuttling (Scheme 2). $FemX_{Wv}$ catalyzes alanyl transfer from the 2′ position of Ala-$tRNA^{Ala}$ whereas peptidyl transfer occurs from the 3′ position in the ribosome,[15–18] indicating that the 2′- and 3′-hydroxy groups of A^{76} have inverse roles in these reactions. The tetrahedral intermediate is stabilized by a protein residue (Lys305) in $FemX_{Wv}$ instead of a water molecule oriented by 23S nucleotide residues A2602 and U2584 in the ribosome. This mechanism is clearly different from that of eubacterial leucyl/phenylalanyl-tRNA protein transferase (LF-transferase).[19,20] The latter enzyme catalyzes transfer of Leu or Phe from Leu-$tRNA^{Leu}$ or Phe-$tRNA^{Phe}$ to the *N*-terminal Arg or Lys residue of proteins that are thereby targeted for recognition by the adaptator protein CplS and degradation by the bacterial proteasome-like protease ClpAP21. Peptide-bond formation by LF-transferase involves a classical protein-based mechanism in which an Asp residue assists a Gln residue in the capture of a proton from the α-amino group at the *N*-terminus of the protein for nucleophilic attack of the carbonyl of the aminoacyl-tRNA ester. In contrast, $FemX_{Wv}$ provides a unique environment for substrate-assisted catalysis by constraining Ala-$tRNA^{Ala}$ and UDP-MurNAc-pentapeptide in the reactive conformations for aminoacyl transfer. This mechanism is unique for protein-based peptide bond formation by tRNA-dependent enzymes.

Received: February 28, 2013
Published online: June 6, 2013

Keywords: reaction mechanisms · nucleoprotein complexes · peptidoglycan · peptidyl-RNA conjugates · transferase

[1] J.-L. Mainardi, R. Villet, T. D. Bugg, C. Mayer, M. Arthur, *FEMS Microbiol. Rev.* **2008**, *32*, 386–408.
[2] K. Dare, M. Ibba, *Wiley Interdiscip Rev. RNA* **2012**, *3*, 247–264.
[3] S. Biarrotte-Sorin, A. P. Maillard, J. Delettré, W. Sougakoff, M. Arthur, C. Mayer, *Structure* **2004**, *12*, 257–267.
[4] M. Fonvielle, M. Chemama, M. Lecerf, R. Villet, P. Busca, A. Bouhss, M. Ethève-Quelquejeu, M. Arthur, *Angew. Chem.* **2010**, *122*, 5241–5245; *Angew. Chem. Int. Ed.* **2010**, *49*, 5115–5119.
[5] S. S. Hegde, J. S. Blanchard, *J. Biol. Chem.* **2003**, *278*, 22861–22867.
[6] A. H. El-Sagheer, R. Kumar, S. Findlow, J. M. Werner, A. N. Lane, T. Brown, *ChemBioChem* **2008**, *9*, 50–52.
[7] D. Graber, H. Moroder, J. Steger, K. TrappI, N. Polacek, R. Micura, *Nucleic Acids Res.* **2010** *38*, 3796–6802.
[8] M. Fonvielle, D. Mellal, D. Patin, M. Lecerf, D. Blanot, A. Bouhss, M. Santarem, D. Mengin-Lecreulx, M. Sollogoub, M. Arthur et al., *Chem. Eur. J.* **2013**, *19*, 1357–1363.
[9] C. W. Tornøe, C. Christensen, M. Meldal, *J. Org. Chem.* **2002**, *67*, 3057–3064.
[10] V. V. Rostovtsev, L. G. Green, V. V. Fokin, K. B. Sharpless, *Angew. Chem.* **2002**, *114*, 2708–2711; *Angew. Chem. Int. Ed.* **2002**, *41*, 2596–2599.
[11] R. Villet, M. Fonvielle, P. Busca, M. Chemama, A. P. Maillard, J.-E. Hugonnet, L. Dubost, A. Marie, N. Josseaume, S. Mesnage et al., *Nucleic Acids Res.* **2007**, *35*, 6870–6883.
[12] H. C. Kolb, K. B. Sharpless, *Drug Discovery Today* **2003**, *8*, 1128–1137.
[13] M. Chemama, M. Fonvielle, M. Arthur, J.-M. Valéry, M. Etheve-Quelquejeu, *Chem. Eur. J.* **2009**, *15*, 1929–1938.
[14] A. H. El-Sagheer, A. P. Sanzone, R. Gao, A. Tavassoli, T. Brown, *Proc. Natl. Acad. Sci. USA* **2011**, *108*, 11338–11343.
[15] D. A. Hiller, V. Singh, M. Zhong, S. A. Strobel, *Nature* **2011**, *476*, 236–239.
[16] E. K. Y. Leung, N. Suslov, N. Tuttle, R. Sengupta, J. A. Piccirilli, *Annu. Rev. Biochem.* **2011**, *80*, 527–555.
[17] M. Simonović, T. A. Steitz, *Biochim. Biophys. Acta Gene Regul. Mech.* **2009**, *1789*, 612–623.
[18] T. M. Schmeing, V. Ramakrishnan, *Nature* **2009**, *461*, 1234–1242.
[19] K. Watanabe, Y. Toh, K. Suto, Y. Shimizu, N. Oka, T. Wada, K. Tomita, *Nature* **2007**, *449*, 867–871.
[20] K. Suto, Y. Shimizu, K. Watanabe, T. Ueda, S. Fukai, O. Nureki, K. Tomita, *EMBO J.* **2006**, *25*, 5942–5950.

